Analysis of Ink Ejection Failure in a MEMS Micro-Injector Printing Head

In-Yao Lee, Tsung-Ping Hsu, Wai W Wang, Yi Chiu*, Hua-Kun Tang,
Fan-Chung Tseng, Kelvin Lee

Advanced Technology Center, BenQ Corporation
23 Li-Hsin Road, Hsinchu Science Park, Hsinchu, Taiwan 300, ROC wiss Federal Institute of Technology, DMT-IMS
*Department of Electrical and Control Engineering, National Chiao Tung University
1001 Ta Hsueh Road, Hsinchu, Taiwan 300, ROC

ABSTRACT

The failure mechanism of a monolithic MEMS twin-bubble micro-injector failing to eject ink smoothly is investigated. The nozzle plate structure is insufficient to resist the thermally induced stress, resulting in chamber wall crack and thus ink ejection failure. A stress model is proposed to explain the crack mechanism of this MEMS micro-injector. A solution to eliminate this problem and achieve satisfactory production yield of micro-injector print head is also reported.

Keywords: Inkjet, MEMS, Print Head, Reliability

1 INTRODUCTION

Thermal bubble micro-injectors are being widely used in inkjet printing applications. The reason for the thermal bubble micro-injector to remain dominant in consumer applications is because of its high performance, low cost, and good reliability [1]. The fabrication of a micro-electromechanical-system (MEMS) based thermal micro-injector requires very precise assembly of various components to form the micro-fluidic structure. The micro-injector printing head reported in this paper employs twin bubbles as a virtual valve to eject fluid [2]. An additional thick nozzle plate is electroplated to provide robust support for stable droplet ejection [3]. Further, this thick nozzle plate enhances heat dissipation of this micro-injector to achieve higher printing speed.

In a large scale MEMS printing head factory producing more than one hundred thousand heads per month, cracks in chamber walls and printing failures were observed. This paper describes an investigation to identify the root cause of the crack in the MEMS micro-injector printing head. A stress model is proposed to explain the crack mechanism when the fabricated head is subject to thermal cycling. The investigation demonstrates the effectiveness of the stress analysis to locate the weak spot of structure in the MEMS micro-injector. Based on the model, the design window of the printing head can be found to eliminate the crack problem and printing failure. Yield data showing the effectiveness of the design window is also reported.

2 DEVICE DESIGN AND FABRICATION

The black cartridge of the MEMS micro-injector reported in this paper, as shown in Figure 1, consists of 300 nozzles and is capable of ejecting 3 million droplets per second [4]. The structure of the MEMS printing head is shown in Figure 2. The ink chambers are directly carved in the silicon substrate through chemical etching. The integration is realized by the monolithically fabrication of driving circuitry, manifold, ink chambers, nozzles, and heaters by standard PMOS process followed by MEMS post processing.

The ink is fed through the manifold from the backside of the printing head into individual chambers, where double heaters sit above the chamber with a nozzle opening centered between them. When the paired heaters are driven by a pulsed voltage, double bubbles are activated to expand and expel a single droplet through the nozzle. Then capillary force then takes over to pull the ink in and refill the empty chamber.

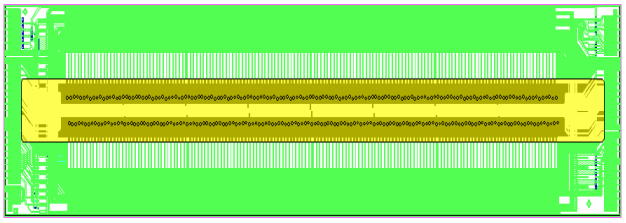

Figure 1: Black printing head of a MEMS micro-injector.

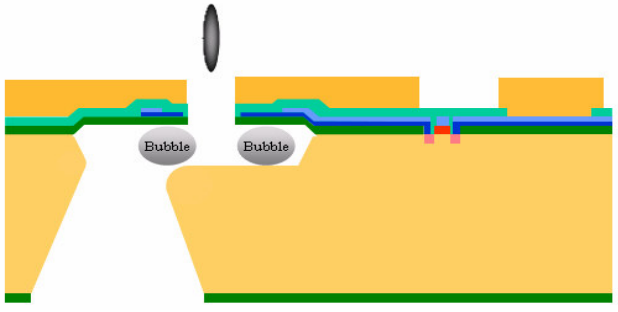

Figure 2: Structure of the MEMS printing head.

To assure highest printing quality, each printing head is subject to ink ejection test to make sure that every nozzle ejects ink smoothly during the printing process. In the printing test, some nozzles on the printing head failed to eject ink. We further observed the ink chambers cracked after the printing head was stressed through a 28-hour thermal cycle. This 28-hour thermal cycle is operated from -25 to 60°C. The temperature is fixed at -25 and 60 °C for 10 hours respectively, whereas both temperature ramp-up and –down, take 4 hours. Figure 3 and Figure 4 show the cracks of the chamber wall in a micro-injector after the thermal cycling.

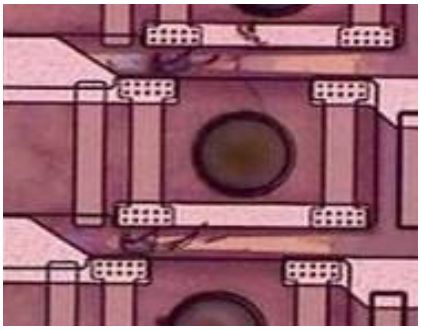

Figure 3: Cracks of the ink chamber in the MEMS micro-injector (gold layer removed).

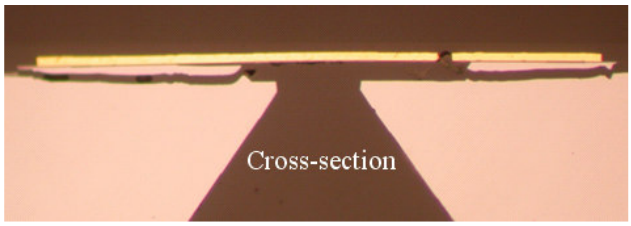

Figure 4: Cross-section view of the ink chamber.

3 MODELING

The cartridge structure of the printing head reported in this study is shown in Figure 5. Polyphenylene Oxide (PPO) is used as the base material of the cartridge housing for its ink compatibility and long term stability. The silicon based MEMS chip containing 300 nozzles and driving circuitry of the printing head is glued onto the cartridge housing directly. The ink is filled into the manifold of the MEMS chip from the backside of the silicon substrate.

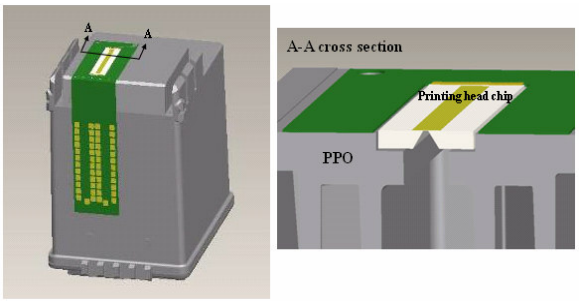

Figure 5: Side view of the printer head cartridge.

The crack of ink chambers occurs while a thermal stress is imposed [5]. From Figure 3 and Figure 4, the crack occurs at the chamber wall, where it is at joint of the silicon substrate and nozzle plate. As can be seen from the schematic structure of the printing head shown in Figure 6, the nozzle plate is a suspended above the manifold and attached to the silicon substrate. The mismatch of thermal expansion among the nozzle plate, the silicon substrate, and the PPO housing induces a stress in the nozzle plate. The suspended nozzle plate bears the thermally induced stress and maintains the integrity of the MEMS structure. In the failure model proposed in this paper, if the thermal stress is larger then the critical threshold, buckling occurs [6] and causes the crack to results in ink ejection failure.

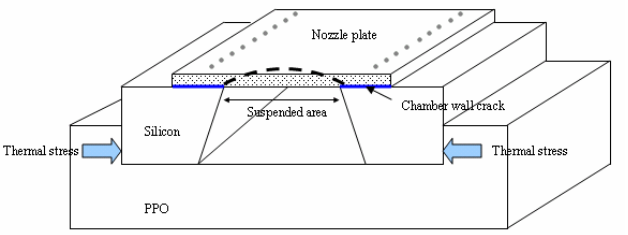

Figure 6: The nozzle plate is suspended on the silicon substrate.

In the nozzle plate shown in Figure 6, the threshold of rigidity critical force of the plate can be expressed as [7]:

$$N_{cr} = \frac{\pi^2 D}{b^2}\left(\frac{b}{a}+\frac{a}{b}\right)^2 \quad \text{(N/m)} \qquad (1)$$

where a and b are the width and length of nozzle plate suspension area, respectively. D is the flexural rigidity of the plate:

$$D = \frac{E_N t_1^{\,3}}{12\left(1-\nu_N^{\,2}\right)} \quad \text{(N·m)} \qquad (2)$$

where E_N is the Young's modulus of the nozzle plate, ν_N is the Poisson's ratio, and t_1 is the thickness of the nozzle plate. The rigidity critical force N_{cr} is closely relative to the dimensions as well as the material characteristics of the

nozzle plate. In the MEMS micro-injector, the width of the nozzle plate is 260μm and it is much smaller than the length 16000μm, that is a << b, Eq. (1) can be simplified as:

$$N_{cr} = \frac{\pi^2 D}{a^2} \quad \text{(N/m)} \qquad (3)$$

When the thermal stress is larger than the threshold of critical rigidity of the MEMS structure, the nozzle plate is starting buckling and ink chamber wall collapses. The larger the rigidity critical force, the more robust the nozzle chamber of the micro-injector. We use this rigidity critical force as a critical parameter to analyze the strength of the ink chamber structure of the MEMS micro-injector. Figure 7 shows the layer structure of the nozzle plate. Table 1 shows the mechanical properties of each layer of the nozzle plate.

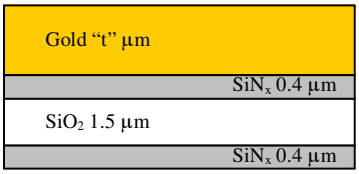

Figure 7: Nozzle plate layer structure

Material	Young's Modulus E (Pa)	Poisson's ratio ν	Thickness t (μm)	CTE ($1/^\circ C$)
Silicon	1.3×10^{11}	0.278	675	3.61×10^{-6}
SiN_x	2.9×10^{11}	0.24	1.2	2.8×10^{-6}
SiO_2	6.8×10^{10}	0.19	1.5	0.75×10^{-6}
Gold	7.72×10^{10}	0.42	t	14.6×10^{-6}
PPO	2.4×10^{9}		1000	70×10^{-6}

Table 1: Material property [8]

Because the silicon substrate is much thicker than the nozzle plate and the Young's modulus of the silicon substrate is much greater than that of the PPO housing, we thus simplify the modeling by ignoring the silicon deflection and stress effect on the nozzle plate from the PPO housing directly. The shear force at the substrate-plate interface and the resulted stress gradient in the nozzle plate are also ignored. Therefore, the force model can be simplified as shown in Figure 8.

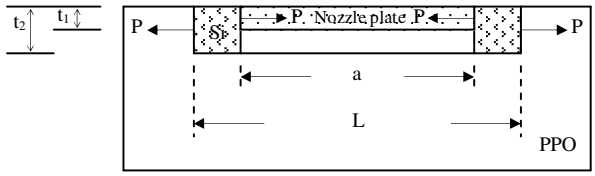

Figure 8: Thermal deformation and force model.

Based upon the situation of static equilibrant among each layer,

$$\alpha_{PPO}\cdot\Delta T\cdot L-\frac{PL}{bt_2\cdot E_{PPO}}=\alpha_N\cdot\Delta T\cdot a+\frac{Pa}{bt_1\cdot E_N} \qquad (4)$$

where α_i is the CTE of layer i, △T is the temperature variation (-25 to 60 ˚C), t_2 and L are the depth and width of PPO housing fillister, and P is the thermal induced force experienced from the mismatch between nozzle plate and PPO housing. Based upon the parameters listed in Table 1, we can solve the force equations to obtain the thermal induced force.

The force imposed on the nozzle plate N_w due to the thermal stress can be expressed as:

$$N_w = \frac{P}{b} \quad \text{(N/m)} \qquad (5)$$

To prevent buckling of the nozzle plate, the thermally induced force should not exceed the threshold of the critical rigidity of the nozzle plate. For a stable MEMS structure in the thermal cycling,

$$N_w \le N_{Cr} \qquad (6)$$

Thus, from Eqs. (1), (4), (5), and (6), we can obtain the constraint of the MEMS structure:

$$\frac{22.53\cdot a^2}{(179.57t+1046.7+a)\cdot(t+2.7)^2}\le 1 \qquad (7)$$

Besides the constraint of critical rigidity, to assure smooth operation of ink droplet ejection and refill, the minimum manifold opening should be at least 10 times larger than the volume of one droplet. Further, for a 600dpi resolution print head to achieve the printed dot size of 60 μm, a nozzle diameter of 32 μm is used in the MEMS device in this paper. Thus, the manifold opening is at least 190 μm for a robust structure design.

On the other hand, the gold layer thickness of the nozzle plate cannot be thicker than 20 μm due to the nozzles cannot be completely opened by the reactive ion etch (RIE) process. Based upon the constraints imposed by the critical rigidity, RIE dry etching limitation, and printing resolution, the ink chamber design constrains safety region is illustrated in Figure 9.

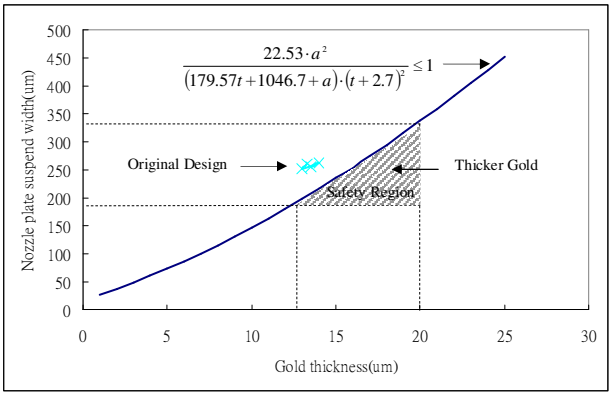

Figure 9: Design constraint of MEMS

4 EXPERIMENTAL RESULT AND DISCUSSION

Based upon the above modeling, the robustness of the chamber strongly depends upon the mechanical strength of the nozzle plate and the opening size of the manifold. To enhance the critical rigidity of the nozzle plate in the MEMS micro-injector, the opening size of the manifold is optimized at 230 μm, and gold layer thickness of the nozzle plate is enhanced from 13μm to 17μm to strengthen the thermal deflection resistance. With the design enhancements, the production yield of MEMS printing head has been substantially improved from 62% to be over 99%, as shown in Table 2. These MEMS printing heads passed the thermal stress test and none of them shows ink ejection failure due to ink chamber crack.

In the stress model proposed in this paper, we ignore the residual stress of each layer with nozzle plate based upon the measurement data as shown in Table 3. The residual stress is much smaller than that of thermal stress from PPO housing (~9000N/m).

Lot No	Gold thickness(μm)	Nozzle plate suspended width(μm)	Quantity	Defect number	Yield rate
A	13.5	255	75	28	62.67%
A	14	262	142	66	53.52%
B	13	251	110	37	66.36%
B	13.3	260	93	32	65.59%
A	17.1	260	306	1	99.67%
A	17.2	255	519	5	99.04%
B	17.5	262	193	0	100.00%
B	17.2	248	191	1	99.48%

Table 2: Production yield of printing head without/with design enhancement.

Material \ Items	Thickness (μm)	Residual Stress (N/m)
Silicon wafer	675	0
SiN_x	1.2	117.02
SiO_2	1.5	-9.41
Gold after anneal	13	670.8

Table 3: Measured residual stress of each layer in nozzle plate (by Tencor FLX-2320)

5 CONCLUSION

The failure mechanism of a monolithic MEMS twin-bubble micro-injector failed to eject ink smoothly has been investigated. A model to analyze the thermal expansion miss-match among the nozzle plate, the silicon substrate, and the PPO housing is also proposed to explain the failure mechanism of the MEMS micro-injector printing head. In the proposed model, the thickness of nozzle plate and the width of manifold opening are the key parameters to be carefully considered to achieve a robust design of the MEMS structure reported in this paper. When the gold layer thickness of nozzle plate is increased to 20 um, the robustness of the MEMS structure is improved substantially and no more ink ejection failures related to chamber crack of thermal stress is observed.

REFERENCES

[1] H.P. Lee, Progress and trends in ink-jet printing technology, Journal of Imaging Science and Technology, Vol.42 No.1 (1998), 49-62.

[2] C. J. Kim, F. G. Tseng, C. M. Ho, United States Patent No. 6,273,553, Aug 2001.

[3] H. S. Hu, W. L. Chen, I. Y. Lee, T. P. Hsu, C. C. Chou, S. S. Wu, United States Patent No. 7,040,740, May 2006.

[4] C.C. Chen, T.W. Huang, United States Patent No. 6,471,338, October 2002.

[5] J. P. Holman, "Heat Transfer", McGraw-Hill International Editions, 1997.

[6] D. O. Brush and B. O. Almroth, "Buckling of Bars, Plates, and Shells", McGraw Hill, New York, 1975

[7] A. C. Ugural, "Stresses in Plates and Shells", McGraw-Hill International Editions, 1999.

[8] MatWeb, material property data http://www.matweb.com